Nanoscale

Cite this: *Nanoscale*, 2011, **3**, 1451

www.rsc.org/nanoscale

COMMUNICATION

Photosensitizer-doped conjugated polymer nanoparticles with high cross-sections for one- and two-photon excitation†

Jennifer L. Grimland,[a] Changfeng Wu,[ab] Ria R. Ramoutar,[ac] Julia L. Brumaghim[a] and Jason McNeill*[a]

Received 5th November 2010, Accepted 24th December 2010
DOI: 10.1039/c0nr00834f

We report a novel nanoparticle that is promising for photodynamic therapy applications, which consists of a π-conjugated polymer doped with a singlet oxygen photosensitizer. The nanoparticles exhibit highly efficient collection of excitation light due to the large excitation cross-section of the polymer. A quantum efficiency of singlet oxygen production of 0.5 was determined. Extraordinarily large two-photon excitation cross-sections were determined, indicating promise for near infrared multiphoton photodynamic therapy. Gel electrophoresis of DNA after near-UV irradiation in the presence of nanoparticles indicated both purine base and backbone DNA damage.

Photodynamic therapy (PDT) is a promising approach to cancer treatment in which a photosensitizer dye, upon exposure to light of the required wavelength, generates reactive oxygen species (ROS) such as singlet oxygen ($^1O_2$) and various radical species, which damage cells by a number of mechanisms including lipid peroxidation and DNA damage, resulting in cell death.[1] In principle, PDT can destroy targeted tissue with reduced collateral tissue damage as compared to other therapies, since both the light and the photosensitizer are required to generate ROS, and the ROS are typically short-lived. In addition, some photosensitizers have been observed to preferentially collect in some types of diseased tissue, resulting in additional improvements in the selectivity of PDT.[2,3] There has also been interest in improving drug targeting by conjugating a photosensitizer to a molecule that binds to receptors that are overexpressed in cancerous tissue.[1,4,5]

There is considerable recent interest in the development of photosensitizers that deliver more ROS for a given dose of light, as well as photosensitizers that are efficiently excited *via* two-photon excitation. Several recent efforts have focused on the development of nanoparticle-based photosensitizing agents, due to their larger one-photon and two-photon optical cross-sections as compared to conventional dyes, as well as the possibility of developing bio-conjugated nanoparticles with enhanced selectivity towards cancerous tissue.[6–13] Recently, we determined extraordinarily large one-photon and two-photon excitation cross-sections for conjugated polymer nanoparticles (CP dots),[14–17] as well as efficient intra-particle energy transfer from the conjugated polymer donor to a variety of polymer or dye acceptors.[15,18,19] These nanoparticles have also been shown to be relatively non-toxic.[20,21] We propose a novel type of photosensitizer nanoparticle composed of a CP dot doped with a photosensitizer dye. We prepared CP dot nanoparticles using tetraphenyl porphyrin (TPP) as the dopant and various conjugated polymers as the host (chemical structures shown in Fig. 1a). The TPP-doped CP dot nanoparticles are relatively small (~50 nm) and form a stable colloidal suspension in water. Upon optical excitation, the conjugated polymer efficiently transfers energy to the porphyrin

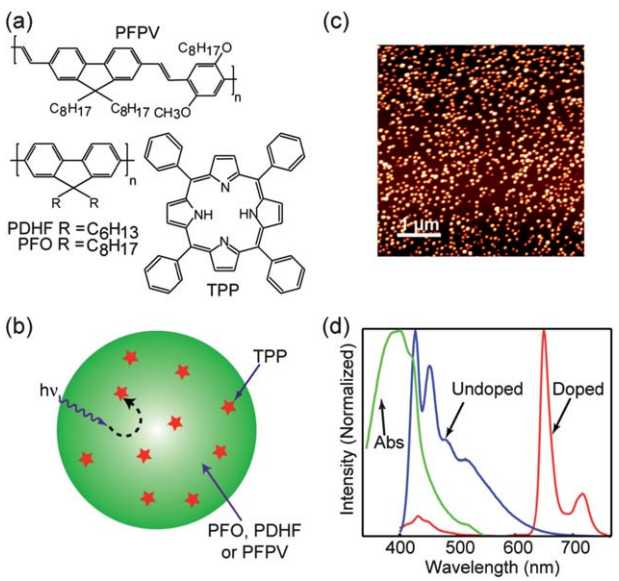

Fig. 1 (a) Chemical structures of the conjugated polymer PDHF and photosensitizer TPP. (b) Nanoparticle representation indicating energy transfer to dopant. (c) A typical AFM image of PDHF dots doped with 10% TPP. (c) Normalized absorbance PDHF doped with 10% TPP (green), fluorescence emission of pure PHDF (blue), and fluorescence emission of PDHF doped with 10% TPP (red).

[a]*Department of Chemistry, Clemson University, Clemson, South Carolina, 29634, USA. E-mail: mcneill@clemson.edu*
[b]*Department of Chemistry, University of Washington, Seattle, Washington, USA*
[c]*Department of Chemistry, Georgia Southern University, Statesboro, Georgia, USA*

† Electronic supplementary information (ESI) available: Fluorescence lifetime determination, AFM particle height histogram, and gel electrophoresis details. See DOI: 10.1039/c0nr00834f

sensitizer (Fig. 1b), resulting in a high singlet oxygen quantum yield in the presence of dissolved molecular oxygen, as determined by the RNO bleaching method.[22] UV irradiation of DNA in the presence of TPP-doped CP dots resulted in extensive oxidative damage to the purine bases and backbone. A key feature of the CP dot nanoparticles is their extraordinarily large two-photon excitation cross-sections given their small size. Both large two-photon excitation cross-sections and efficient singlet oxygen generation were observed for TPP-doped CP dots, which is promising for multiphoton photodynamic therapy applications. Furthermore, CP dot photosensitizers can readily be prepared in various sizes and encapsulated and functionalized to impart improved biocompatibility and specificity for diseased tissue.

The conjugated polymers poly(9,9-dihexylfluorene) (PDHF, M_w 55 000, polydispersity 2.7), poly(9,9-dioctylfluorenyl-2,7-diyl) (PFO, M_w 147 000, polydispersity 3.0) and poly[{9,9-dioctyl-2,7-divinylene-fluoreneylene}-*alt*-*co*-{2-methoxy-5-(2-ethylhexyloxy)-1,4-phenylene}] (PFPV, M_w 270 000, polydispersity 2.7) were all purchased from ADS dyes (Quebec, Canada). Tetrahydrofuran (THF, inhibitor-free, anhydrous, 99.9%), tetraphenylporphyrin (TPP), Rose Bengal (RB), sodium azide (NaN_3), and *p*-nitrosodimethylaniline (RNO) were purchased from Sigma-Aldrich, and imidazole was purchased from Fluka. All reagents were used as provided without further purification. Stable aqueous suspensions of TPP-doped CP dots were prepared by a reprecipitation method described previously.[14,16,18] Briefly, stock solutions were prepared by separately dissolving the conjugated polymer and TPP in THF and stirred overnight, followed by filtration through a 1.6 μm filter. A dilute solution of the conjugated polymer and TPP dissolved in tetrahydrofuran (9 : 1 polymer : TPP weight ratio, 10 ppm solution) is rapidly mixed with water and briefly sonicated to yield a suspension of nanoparticles. Next, 2 mL of the solution was injected into 8 mL of deionized water under sonication, followed by vacuum evaporation to remove the majority of the THF. Finally, the solution was filtered through a 0.2 μm filter to remove any aggregates. The particle size distribution was determined by atomic force microscopy (AFM) as follows. The nanoparticle suspension was drop-cast onto a clean glass substrate. The samples were then imaged using an Ambios Q250 AFM in AC mode, at a pixel resolution of 10 nm. The particle height was used as a measure of the particle diameter, since previous results have shown these nanoparticles to be approximately spherical.

A spectrophotometric method was employed to determine the $^1O_2$ quantum yield.[22] The method is described briefly as follows. A buffered solution containing the photosensitizer, RNO, and imidazole is irradiated with light, resulting in the formation of $^1O_2$. Imidazole reacts with singlet oxygen to form a transannular peroxide species that subsequently oxidizes RNO, and the depletion of RNO is monitored by UV-Vis spectrometry at 440 nm. Rose Bengal (RB) was employed as the standard for the determination of singlet oxygen quantum yield. The irradiation was carried out in a commercial fluorimeter (Quantamaster, PTI, Inc.) employing a 75 W Xe lamp, with the excitation set to match the peak absorbance of the polymer of interest, and the RNO absorbance was monitored at ten minute intervals using a Shimadzu UV-2101PC scanning spectrophotometer (Fig. 2a). The mixture of RNO, imidazole, and TPP-doped nanoparticles was stirred constantly during irradiation. Determination of the relative singlet oxygen quantum yield $\Phi(^1O_2)$ from the photobleaching kinetics data was performed as follows. The kinetics analysis is based on the rate equation,[22]

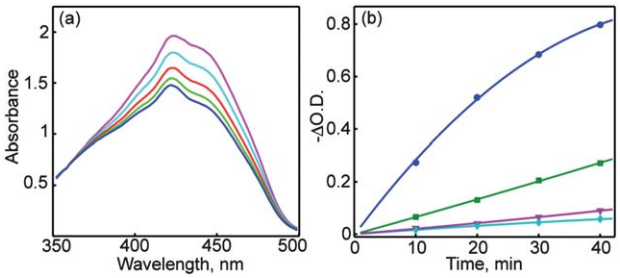

Fig. 2 (a) Stacked spectra showing successive depletion of RNO with irradiation time. (b) RNO depletion by $^1O_2$ with 6 mM imidazole monitored at 440 nm in 50 mM (pH 7.4) phosphate buffer with TPP doped PDHF (●), PDHF (■)PDHF-TPP, in the presence of 6 mM NaN_3 (▼), PDHF-TPP in the absence of imidazole (◆).

$$-\frac{d[RNO]}{dt} = I_{ab}\Phi(^1O_2)\frac{k_r[RNO]}{k_d}$$

where k_r and k_d are the rate constants for chemical quenching of singlet oxygen by RNO and chemical deactivation of singlet oxygen by the solvent, respectively, and I_{ab} is the intensity of light absorbed by the sample or standard. A straight line was fit to a plot of $-\ln A_{RNO}(t)/A_{RNO}(0)$ *versus* t for both standard and nanoparticle samples, resulting in a slope of $I_{ab}\Phi(^1O_2)(k_r/k_d)$. The singlet oxygen quantum yield is known for the standard and I_{ab} was measured for both the standard and the nanoparticle absorption wavelengths.[23] Since the initial concentrations of RNO were constant across all samples, the singlet oxygen quantum yield of the nanoparticle samples is determined using the expression,

$$\Phi(^1O_2)_{np} = \Phi(^1O_2)_{std} \times \frac{k_{np}}{k_{std}}$$

where k_{np} and k_{std} are obtained from the slopes of the first order kinetics plots, corrected for absorbance. The rate of bleaching of RNO at 440 nm as a function of irradiation time for the various assays is shown in Fig. 2b.

In addition, the fluorescence lifetime of the TPP excited state in the TPP-doped PDHF nanoparticles was determined, and gel electrophoresis was performed to quantify DNA backbone and base damage by singlet oxygen and ROS generated by irradiation of TPP-doped PDHF nanoparticles. Additional information about the fluorescence lifetime experiments and gel electrophoresis experiments is provided in the ESI†.

The two-photon excitation cross-section of TPP doped PFPV nanoparticles at an excitation wavelength of 800 nm was determined as follows. A passively mode-locked Ti:sapphire laser (Coherent, Mira, 800 nm, ~100 fs), focused using an 30 mm focal length achromat lens, was used as the excitation source. The nanoparticle suspension was placed in a 1 cm quartz cuvette located at the focus of the laser. The fluorescence was collected at 90° using a 30 mm focal length lens, filtered through a pair of 700 nm shortpass dielectric filters and a Schott BG-38 colored glass filter to remove scattered laser light, and subsequently focused onto a single photon avalanche photodiode module (Quantique id100-50). The excitation power was varied from 50 mW to 100 mW and the resulting fluorescence intensity was recorded. The two-photon fluorescence cross-section was determined using the expression,

$$\langle F(t)\rangle \approx \frac{1}{2}\eta C\sigma^*_{2p}\frac{g_p}{f\tau}\frac{8n\langle P(t)\rangle^2}{\pi\lambda}$$

where $\langle F(t)\rangle$ is the fluorescence intensity; η is the fluorescence collection efficiency of the instrument; C is the concentration of the TPP doped PFPV system; σ^*_{2p} is two-photon action cross-section of the system; g_p is a dimensionless constant related to pulse shape and optical setup; f is the laser repetition rate; τ is the width of the laser pulse; n is the refractive index of the focusing lens; λ is the wavelength of the laser and $\langle P(t)\rangle$ corresponds to laser power. A plot of $\log\langle F(t)\rangle$ *versus* $\log\langle P(t)\rangle$ resulted in a straight line with a slope of slightly less than two, indicating two-photon excitation. The *y*-intercept, *b*, was recorded for determination of the cross-section. Lucifer yellow in DI water was used as a standard dye[24] for the relative determination of the two-photon action cross-section of the TPP doped PFPV particles, calculated using the expression,

$$\sigma^*_{2p} = \sigma^*_{2p,0}\frac{C_0}{C}\exp(b - b_0)$$

where $\sigma^*_{2p,0}$ refers to the two-photon action cross-section of the standard, C_0 and C are the concentrations of the standard and TPP doped PFPV nanoparticles, respectively (estimated from the peak absorbance and the previously reported extinction coefficient), and b_0 and b are the *y*-intercepts obtained from the log–log plot of laser intensity *versus* fluorescence emission intensity of Lucifer yellow and TPP doped PFPV, respectively.

TPP-doped conjugated polymer nanoparticles were prepared from PDHF, PFO, and PFPV (polymer structures shown in Fig. 1a). Analysis of the particle morphology in the AFM results indicates that the TPP-doped PDHF particles are approximately spherical in shape (Fig. 1c). The particle height histogram on the AFM image showed that the majority of the TPP doped PDHF particles had diameters in the range of 52 ± 9 nm (particle height histogram shown in the ESI†), consistent with roughly spherical nanoparticles. Assuming the particle is spherical with a 25 nm radius and a density of near unity, the mass per particle is $\sim 7 \times 10^{-17}$ g. Given the molecular weights of the polymer and dopant and a doping level of 10 wt%, it is estimated that the particles contain ~600 molecules of PDHF and ~6000 molecules of TPP. Particles of TPP-doped PFO and PFPV yielded particle sizes of 31 ± 7 and 46 ± 10 nm, respectively. The UV-Vis absorption spectra of the TPP-doped PDHF CP dots (Fig. 1d) indicated that the composition of the as-prepared CP dots was consistent with a 9 : 1 weight ratio of PDHF to TPP in the precursor solution. Based on the molar absorptivity of the polymer and particle size, the estimated peak extinction coefficient of the TPP-doped PDHF CP dots (at 377 nm) was $\sim 8.0 \times 10^8$ M^{-1} cm^{-1}, and the estimated absorption cross-section was calculated to be 2.0×10^{-11} cm^2. The energy transfer efficiency from the host CP dots to the TPP dopant was estimated as greater than 95% for all three polymers, as determined from measurements of the host fluorescence intensity F for the doped particles, the fluorescence intensity F_0 of the undoped particles, and the expression $E = 1 - F/F_0$.[18] The observation of high energy transfer efficiency at relatively low ratios of dopant to host polymer provides a clear indication that the TPP co-precipitated within the polymer nanoparticles, since free TPP in solution or substantial segregation of the TPP to form particles consisting primarily of TPP would result in a much lower energy transfer efficiency at the low dye concentrations employed in this study. The fluorescence quantum yield of the TPP in the nanoparticles (exciting primarily the polymer at 400 nm) was determined to be 5.2%, somewhat lower than the fluorescence quantum yield of TPP in an inert polymer matrix,[25] possibly indicating some fluorescence quenching by a fraction of TPP aggregates present within the nanoparticles (which is likely at the TPP fraction employed). The lower fluorescence quantum yield could also be attributed to the fact that the measurement was performed by exciting the nanoparticles at 400 nm, where the absorbance is primarily due to the polymer, and therefore non-radiative relaxation of the polymer excited state would reduce the overall quantum yield. A fluorescence lifetime of 6.1 ns ($\lambda_{ex} = 400$ nm, $\lambda_{em} = 650$ nm, corresponding to TPP fluorescence) was determined by time-correlated single photon counting, which is markedly shorter than the reported lifetime of TPP in toluene,[26] indicating an increased non-radiative rate for TPP, likely due to conformational distortions of the porphyrin (additional information can be found in the ESI†).

The singlet oxygen quantum yield, $\Phi(^1O_2)$, was determined by the RNO bleaching method, using RB as a standard.[22,23] The determined singlet oxygen quantum yield for the TPP-doped PDHF particles ($\Phi(^1O_2) = 0.5$) is similar to that of other good photosensitizers such as RB ($\Phi(^1O_2) = 0.76$),[27] and considerably higher than that of hematoporphyrin in aqueous solution, which exhibits low singlet oxygen yields due to aggregation.[28] While TPP and RB generate primarily singlet oxygen and little other ROS, conjugated polymers can undergo charge transfer and proton transfer reactions in the excited state, which could lead to the production of other ROS (*e.g.*, hydroxyl radicals). In order to estimate the relative production of singlet oxygen *versus* other ROS, additional photobleaching experiments were performed (using TPP-doped PDHF nanoparticles) in the absence of imidazole, which resulted in approximately 80% reduction in the RNO bleaching rate. These results yield an upper bound on the relative amount of photobleaching by other ROS of approximately 20%, indicating that, for the TPP-doped PDHF particles, singlet oxygen is the principal ROS. Undoped PDHF nanoparticles were found to have a singlet oxygen quantum yield of ~0.1, indicating that doping with TPP improves the efficiency of singlet oxygen generation due to efficient energy transfer from the polymer to the TPP and the high triplet yield of TPP.

DNA damage by nanoparticle-generated ROS was measured using gel electrophoresis (Fig. 3). When nanoparticles were combined with DNA without 377 nm irradiation (lane 5), DNA damage was not observed. Increasing the irradiation time of nanoparticles with DNA (50–200 min) resulted in increasing DNA damage (lanes 6–8). Quantification of the gel bands indicated that irradiation times of 100 and 200 min produced approximately 50% and 79% backbone-damaged DNA, respectively. To determine purine base damage, gel electrophoresis experiments were conducted with the Fpg enzyme that nicks DNA at oxidized guanine and adenine bases. Increased

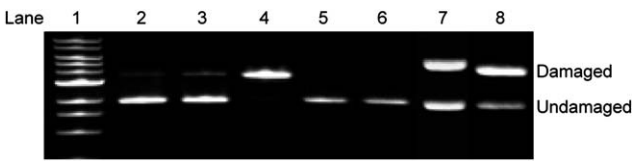

Fig. 3 Electrophoresis gel image showing DNA damage by nanoparticle-generated ROS. Lane 1: 1 kb M_w ladder, lanes 2–4: plasmid DNA; DNA + H_2O_2 (50 μM); DNA + Fe^{2+} (2 μM) + H_2O_2. Lanes 5–8: DNA + nanoparticles irradiated for 0, 50, 100 and 200 min, respectively.

DNA purine base damage was also observed with increasing irradiation time (50–200 min) for the nanoparticle DNA solutions (data not shown, additional information can be found in the ESI†).

Recently, we have shown that nanoparticles comprised of PFPV copolymer exhibit two-photon absorption cross-sections an order of magnitude larger than nanoparticles composed of conjugated homopolymers such as PDHF, owing to the alternating donor–π–donor structure along the polymer backbone.[16] Therefore, TPP-doped PFPV particles were selected for determination of two-photon cross-section. The two-photon fluorescence cross-section of the TPP doped PFPV CP dots was determined to be 5×10^5 GM (Fig. 4), similar to our previously reported value of undoped PFPV, indicating that the presence of TPP does not significantly change the two-photon cross-fluorescence cross-section.[16] A figure of merit that could be useful for comparing different two-photon PDT agents is the two-photon action cross-section for the generation of singlet oxygen, which can be estimated as the product of the two-photon absorption cross-section and the singlet oxygen quantum yield. Since the singlet oxygen quantum yield of the TPP-doped particles is more than a factor of 2 higher than the fluorescence quantum yield, we estimate a two-photon action cross-section for the generation of singlet oxygen of $\sim 10^6$ GM.

In conclusion, novel nanoparticle photosensitizers have been developed that exhibit very high excitation cross-sections (10^{-15} to 10^{-12} cm^2 for one-photon excitation and $\sim 10^6$ GM for two-photon excitation, depending on polymer and particle size) and high quantum efficiency for singlet oxygen generation. The singlet oxygen quantum yield in aqueous solutions was determined to be ~0.5 for PHDF dots doped with TPP, ~0.3 for PFO dots doped with TPP, and ~0.2 for PFPV dots doped with TPP. In contrast, photosensitizers based on CdTe quantum dots have a similar singlet oxygen quantum yield, but an excitation cross-section more than two orders of magnitude lower than that of CP dots.[29] While there are a number of other reports of a variety of nanoparticles loaded or functionalized with photosensitizers,[13,30] no other reported nanoparticle in this size range appears to possess the combination of high excitation cross-section, high singlet oxygen quantum yield, and small size afforded by the doped CP dots. The relatively high singlet oxygen quantum yield and extraordinarily high light-gathering power of these nanoparticles are highly promising for photodynamic therapy applications, and could lead to large reductions in either the photosensitizer dosing or UV irradiation levels required for effective photodynamic action. Furthermore, the extraordinarily large two-photon excitation cross-sections for the generation of singlet oxygen are well above the suggested threshold for clinical viability for multiphoton-excited photodynamic therapy,[31] which is a promising strategy for more accurate targeting of diseased tissue.[7] Also, encapsulation[32] and bioconjugation of the CP dot nanoparticles to target diseased tissue is a promising strategy towards improving the solubility, efficacy and specificity of photodynamic therapy based on such nanoparticles.

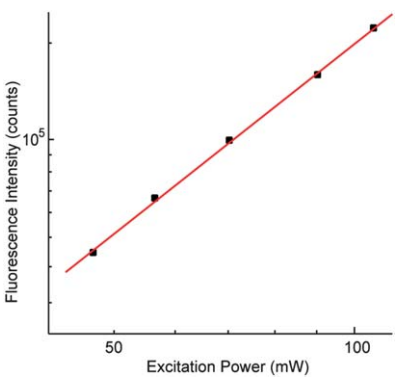

Fig. 4 log–log plot of the fluorescence intensity of the TPP doped PFPV nanoparticles *vs.* the laser power at 800 nm. The slope obtained was 1.94, indicating two-photon excitation. The intercept yields a two-photon fluorescence cross-section of 5×10^5 GM.

Acknowledgements

The authors gratefully acknowledge financial support from the NSF under Grant no. CHE-0547846 (CAREER). The authors also acknowledge the use of specialized equipment purchased with the support of NSF/EPSCoR under Grants no. 2001RII-EPS-0132573 and 2004RII-EPS-0447660.

Notes and references

1 D. E. J. G. J. Dolmans, D. Fukumura and R. K. Jain, *Nat. Rev. Cancer*, 2003, **3**, 380.
2 B. W. Henderson and T. J. Dougherty, *Photochem. Photobiol.*, 1992, **55**, 145.
3 T. J. Dougherty, *Photochem. Photobiol.*, 1987, **45**, 879.
4 Y. N. Konan, R. Gurny and E. Allemann, *J. Photochem. Photobiol., B*, 2002, **66**, 89.
5 S. Verma, G. M. Watt, Z. Mal and T. Hasan, *Photochem. Photobiol.*, 2007, **83**, 996.
6 I. Roy, T. Y. Ohulchanskyy, H. E. Pudavar, E. J. Bergey, A. R. Oseroff, J. Morgan, T. J. Dougherty and P. N. Prasad, *J. Am. Chem. Soc.*, 2003, **125**, 7860.
7 S. Kim, T. Y. Ohulchanskyy, H. E. Pudavar, R. K. Pandey and P. N. Prasad, *J. Am. Chem. Soc.*, 2007, **129**, 2669.
8 J. R. McCarthy, J. M. Perez, C. Bruckner and R. Weissleder, *Nano Lett.*, 2005, **5**, 2552.
9 A. C. S. Samia, X. B. Chen and C. Burda, *J. Am. Chem. Soc.*, 2003, **125**, 15736.
10 D. Gao, R. R. Agayan, H. Xu, M. A. Philbert and R. Kopelman, *Nano Lett.*, 2006, **6**, 2383.
11 S. Dayal and C. Burda, *J. Am. Chem. Soc.*, 2008, **130**, 2890.
12 Y. Cheng, A. C. Samia, J. Li, M. E. Kenney, A. Resnick and C. Burda, *Langmuir*, 2010, **26**, 2248.
13 Y. Cheng, A. C. Samia, J. D. Meyers, I. Panagopoulos, B. W. Fei and C. Burda, *J. Am. Chem. Soc.*, 2008, **130**, 10643.
14 C. Szymanski, C. F. Wu, J. Hooper, M. A. Salazar, A. Perdomo, A. Dukes and J. McNeill, *J. Phys. Chem. B*, 2005, **109**, 8543.
15 C. F. Wu, H. S. Peng, Y. F. Jiang and J. McNeill, *J. Phys. Chem. B*, 2006, **110**, 14148.
16 C. F. Wu, C. Szymanski, Z. Cain and J. McNeill, *J. Am. Chem. Soc.*, 2007, **129**, 12904.
17 C. Wu, B. Bull, C. Szymanski, K. Christensen and J. McNeill, *ACS Nano*, 2008, **2**, 2415.
18 C. F. Wu, Y. L. Zheng, C. Szymanski and J. McNeill, *J. Phys. Chem. C*, 2008, **112**, 1772.
19 C. F. Wu, B. Bull, K. Christensen and J. McNeill, *Angew. Chem., Int. Ed.*, 2009, **48**, 2741.
20 C. F. Wu, T. Schneider, M. Zeigler, J. B. Yu, P. G. Schiro, D. R. Burnham, J. D. McNeill and D. T. Chiu, *J. Am. Chem. Soc.*, 2010, **132**, 15410.
21 L. P. Fernando, P. K. Kandel, J. B. Yu, J. McNeill, P. C. Ackroyd and K. A. Christensen, *Biomacromolecules*, 2010, **11**, 2675.
22 I. Kraljić and S. El Moshni, *Photochem. Photobiol.*, 1978, **28**, 577.
23 E. Gandin, Y. Lion and A. Vandevorst, *Photochem. Photobiol.*, 1983, **37**, 271.
24 C. Xu and W. W. Webb, *J. Opt. Soc. Am. B*, 1996, **13**, 481.
25 B. P. Lyons and A. P. Monkman, *Phys. Rev. B: Condens. Matter Mater. Phys.*, 2005, **71**, 235201.

26 S. Gentemann, C. J. Medforth, T. P. Forsyth, D. J. Nurco, K. M. Smith, J. Fajer and D. Holten, *J. Am. Chem. Soc.*, 1994, **116**, 7363.
27 R. W. Redmond and J. N. Gamlin, *Photochem. Photobiol.*, 1999, **70**, 391.
28 C. Tanielian, C. Schweitzer, R. Mechin and C. Wolff, *Free Radical Biol. Med.*, 2001, **30**, 208.
29 L. X. Shi, B. Hernandez and M. Selke, *J. Am. Chem. Soc.*, 2006, **128**, 6278.
30 D. B. Tada, L. L. R. Vono, E. L. Duarte, R. Itri, P. K. Kiyohara, M. S. Baptista and L. M. Rossi, *Langmuir*, 2007, **23**, 8194.
31 A. Karotki, M. Khurana, J. R. Lepock and B. C. Wilson, *Photochem. Photobiol.*, 2006, **82**, 443.
32 C. F. Wu, C. Szymanski and J. McNeill, *Langmuir*, 2006, **22**, 2956.